Surface electronic structure of *p*-InP using temperature-controlled surface photovoltage spectroscopy

N. Kinrot and Yoram Shapira*
Department of Physical Electronics, Faculty of Engineering, Tel-Aviv University, Ramat-Aviv 69978, Israel
(Received 26 November 2001; published 28 May 2002)

Samples of *p*-InP (100) have been investigated using temperature-controlled surface photovoltage spectroscopy (*T*-SPS), in conjunction with time-resolved photoluminescence and intensity-resolved surface photovoltage measurements. In addition to the previously reported three gap states, attributed to excess surface P, adsorbed O, and Fe unintentional doping, *T*-SPS reveals a gap state, also attributed to Fe, situated 0.79 eV below the conduction-band minimum. The energy distribution of the latter state has been investigated by measuring its population as a function of temperature and shows good agreement with theory. A direct observation of the spectral blueshift of the InP band gap by *T*-SPS shows very good agreement with theory.

DOI: 10.1103/PhysRevB.65.245303 PACS number(s): 73.20.At, 71.55.Eq, 78.66.Fd

I. INTRODUCTION

InP-based devices have become dominant in a number of microelectronic[1] and optoelectronic[2] device technologies. In several reviews on InP-based devices and applications,[3–6] fast response heterojunction bipolar transistors, high electron mobility transistors, advanced chip integration and fabrication are discussed. Other topics include the nature of InP and its application to nanoscale electronics and optoelectronics.[4] Further advances in understanding the physical nature of InP have been extensively reported.[7,8] In view of this intense current interest in InP, there is an obvious need for information on its surface electronic properties.

In this paper we try to achieve several goals. One is obtaining the energy distribution of a gap state, using the Fermi-level shift induced by temperature-controlled surface photovoltage spectroscopy (*T*-SPS) measurements. Another goal is using the effect of temperature-controlled measurements on the SPS sensitivity and directly observing the ''spectral blueshift,'' i.e., widening of the band gap at lower temperatures.

The measurement setup and procedures are described in the following section. The following section includes the suggested rational for the energy positioning of the two Fe-induced surface states, the description of the temperature effect on the band-to-band transition surface photovoltage (SPV) signal, and the spectral blueshift quantification. The conclusion section abbreviates the discussion and its repercussions. Appendix A contains the detailed Shockley-Read-Hall (SRH) treatment of the $E_C-0.79$ eV state, and a procedure for calculating the Fermi and valence-band positions, relative to the intrinsic Fermi level, as a function of temperature.

II. EXPERIMENTAL

The substrates used were (100)-oriented Zn-doped (6.7×10^{16} cm^{-3}) *p*-InP wafers supplied by Crismatec (InPact), France. The wafers were liquid encapsulated Czochralski grown. Prior to the measurements every sample was etched by a 1:1:2 HCl (36.46%): HNO_3 (65%): H_2O (doubly distilled) solution for 20 s, rinsed in doubly distilled water, and dried in ambient air.

The surface electronic structure of the samples has been investigated by SPS.[9] SPS is a well-established method for detection of the energy position of local states inside a semiconductor band gap. The SPV is monitored using a commercial kelvin probe unit (Besocke Delta Phi, Germany) with a ~1 mV sensitivity.[10] The samples under investigation are illuminated from the etched side through a 0.25-m grating monochromator fed by a 250-W tungsten-halogen lamp. The output illumination power at the sample surface typically lies in the microwatt region.

For *T*-SPS measurements, the sample and probe were situated in a cryostat (Janis) under high vacuum conditions ($\sim2\times10^{-6}$ Torr) to prevent water condensation. The controlled temperature (80–300 K) was monitored using a programmable control unit with a stabilizing capability of ±1 K (Lakeshore). The dewar was vibration-isolated from the turbomolecular pump (ALCATEL, France).

III. RESULTS AND DISCUSSION

Figure 1 shows a room-temperature SPV spectrum of InP (100). The slope changes indicate three gap states, whose position relative to the conduction-band minimum E_C (valence band maximum E_V) can be deduced from the position of the downward (upward) slope changes in the spectrum. Starting at the lower energies, the upward slope change at 1.04 eV indicates population of a donor state, situated at $E_V+1.04$ eV (denoted by D_1 in Fig. 1). This state is attributed to excess surface P.[11–13] The downward slope change at 1.12 eV indicates depopulation of an acceptor state, situated at $E_C-1.12$ eV, (denoted by S_1) and is attributed to unintentional Fe doping.[14,15] The abrupt upward offset at 1.18 eV was verified to appear due to an optical filter change. The next downward slope change indicates depopulation of an acceptor state, situated at $E_C-1.25$ eV (denoted by A_1) and attributed to adsorbed O.[11–13] The major upward slope starting at ~1.3 eV and ending at ~1.35 eV represents the band-to-band transition.

Time-resolved photoluminescence measurements yielded a mean carrier lifetime of ~0.25 ns with no measurable ef-

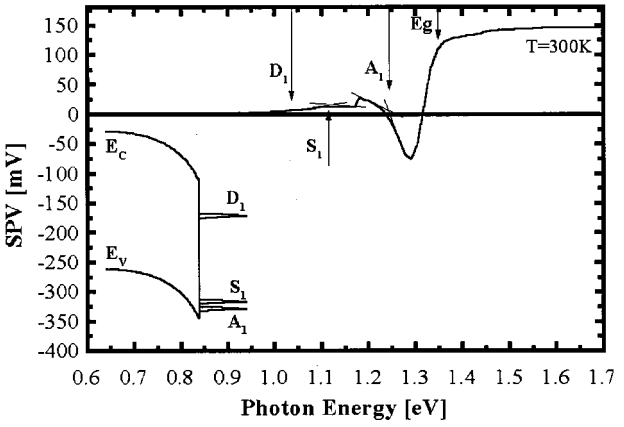

FIG. 1. The SPV spectrum of *p*-InP(100) at room temperature, with the D_1, A_1, and S_1 states pointed out. Inset shows a schematic band diagram.

fect of temperature. Thus, the samples rapidly reach steady state under the microwatt illumination intensity.

Intensity-resolved SPV measurements[16] indicate that A_1 and D_1 are surface states rather than bulk states. The Fe presence at the surface has previously been reported to introduce two states, situated at $E_C-1.12$ eV and $E_C-0.79$ eV.[14,15] In our case, only the former is observed at room temperature. Low-temperature SPV measurements are expected to yield higher sensitivity to surface charge redistribution. This is mainly due to the suppression of lattice phonons and reduction of thermally induced charge-carrier concentration with decreasing temperature, which enhances the influence of the photoinduced carriers.

Figure 2 shows typical SPV spectra of the etched *p*-InP substrates taken at 300, 250, 180, and 150 K. The spectrum at 200 K was omitted for clarity. As temperatures decrease, the onset of the Fe-induced state at $E_C-0.79$ eV (denoted by S_2 in Fig. 2) is clearly observed. Its SPV signal grows with

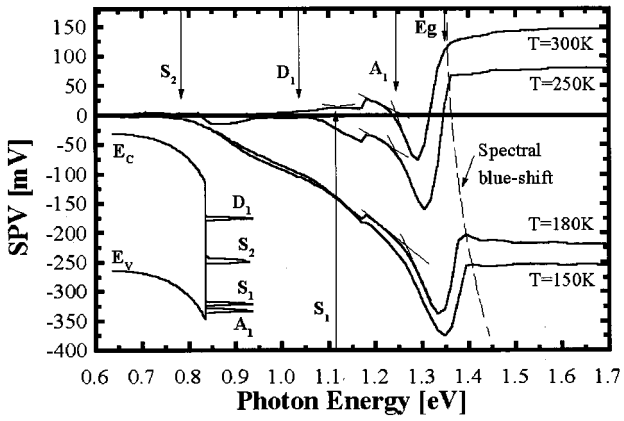

FIG. 2. The SPV spectra of *p*-InP(100) at 300, 250, 180, and 150 K. The Fe-induced $E_C-0.79$ (S_2) and $E_C-1.12$ (S_1) states are depicted. The onset of the S_2 state is clearly observed. Its SPV signal increases with decreasing temperature. The band-to-band transition spectral blueshift is pointed out (dashed curve). Inset: a schematic band diagram.

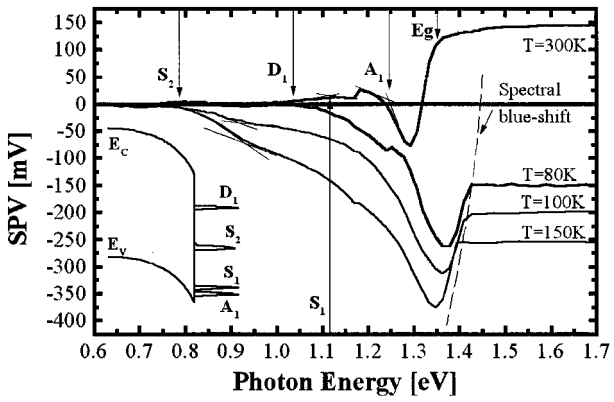

FIG. 3. The SPV spectra of *p*-InP(100) at 300, 150, 100, and 80 K. The Fe-induced $E_C-0.79$ (S_2) and $E_C-1.12$ (S_1) states are depicted. Here, the D_1, A_1, and S_1 states are marked, with no new information except that the S_2 SPV signal *decreases* with decreasing temperature. The band-to-band transition spectral blueshift is pointed out (dashed curve). Inset: a schematic band diagram.

decreasing temperature due to temperature-induced sensitivity enhancement.

The schematic surface band structure appearing in the inset is based on the *bulk* energy positions of the Fermi level and the valence band, relative to the intrinsic Fermi level (see Appendix B). Then, choosing 150 K as a temperature from which to extract the initial surface band bending (under thermal equilibrium), one subtracts the Fermi-level relative position (e.g., 35.7 meV at 150 K) from the energy of the state onset (e.g., 806 meV at 150 K), yielding an initial band bending of $\sim$0.56 eV. The relatively high sub-band gap SPV signal in comparison with the band-to-band transition is attributed to the cummulative influence of active states together with Fermi-level pinning. Figure 3 shows typical SPV spectra of the etched *p*-InP substrates taken at 300, 150, 100, and 80 K. The temperature spectrum at 120 K was omitted for clarity. Here, the D_1, A_1, and S_1 states are present, but contain no new information. However, the S_2 SPV signal *decreases* with decreasing temperature, indicating the dominance of another mechanism.

Let us consider a situation in which a significant depopulation of the S_2 state occurs only at temperatures below 150 K. Such a situation may occur due to a temperature-induced shift of the quasi-Fermi level across the state. In this case, as long as the state is almost fully populated (at temperatures above 150 K in Fig. 2), we observe the sensitivity-enhanced signal. But, as soon as significant depopulation of the state occurs, we observe a diminishing S_2 SPV signal as temperatures continue to decrease.

To try explaining this phenomenon, we turn to SRH statistics, applied to the description of the surface-state population.[9] Based on the theoretical analysis, presented by Kronik and Shapira, the SRH presentation for a surface-state normalized population, under steady-state illumination conditions, is

$$\frac{n_t}{N_t}=\frac{C_n n_b e^{qV_S/kT}+C_p p_1}{C_n(n_b e^{qV_S/kT}+n_1)+C_p(p_b e^{-qV_S/kT}+p_1)}. \quad (1)$$

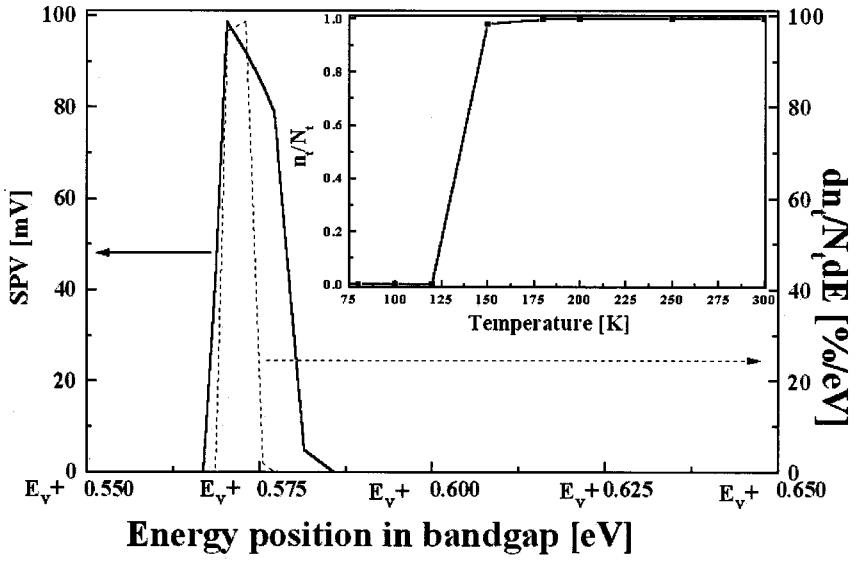

FIG. 4. The SPV signal of the S_2 state, at 1 eV, and the normalized state distribution, as a function of energy. The correlation depicts the S_2 state in its near midgap position. Hence the notation of energy position relative to the valence band. Inset: the normalized population of the state as a function of temperature.

Here, n_t is the population concentration, N_t is the total state concentration, and T is the temperature in degrees Kelvin. C_n and C_p are the electron- and hole-capture cross sections, respectively, while n_1 and p_1 are the fractional populations of the state. The latter refer to the relative position of the S_2 state from the bulk valence and conduction band (outside the space-charge region). n_b and p_b are the bulk thermally induced charge-carrier concentrations. V_S is the band bending at the surface under steady-state illumination conditions (low optical injection conditions). Through V_S the optical electron-hole pair generation is taken into account.[9]

We assume $n_b \approx n_i^2(T)/N_A \ll p_b \approx N_A$ (which, for $N_A = 6.7\times 10^{16}$ cm^{-3}, is safe to assume). After taking note of weakly temperature-dependent variables (a full mathematical description is given in Appendix A), the normalized population may be expressed by

$$\frac{n_t}{N_t} = \frac{\alpha(T)T^{3/2}}{\delta(T)T^{3/2} + \gamma(T)e^{-q\mathrm{SPV}(T)/kT}}. \tag{2}$$

Denoted in Appendix A as Eq. (A6), this expression links our SPV measurements to the SRH-based analysis. Here, $\alpha(T)$, $\gamma(T)$, and $\delta(T)$ are weakly temperature-dependent variables in the relevant temperature range (80–300 K). The first, energy-based derivative of the normalized population yields the state energy distribution and is correlated to the measured S_2 SPV signal.

Figure 4 shows the SPV signal (solid curve) and the energy derivative of the normalized population (dotted curve) of S_2 as a function of energy (with respect to the valence-band maximum at the surface). The former is experimentally taken at 1 eV from spectra, such as in Figs. 2 and 3. This position is not affected by the D_1 state. The inset of Fig. 4 shows the normalized population of the S_2 state [as expressed by Eq. (2)] as a function of temperature. A significant depopulation of the S_2 state begins around ~180 K reaching almost zero near ~120 K. The depopulation occurs due to the shift of the quasi-Fermi level across the state with temperature, reaching approximately complete depopulation.

The correlation between the experimental and calculated lower-energy half of the distribution (the left-hand slope in Fig. 4) is quite good. Our measurements are valid for investigation of the state distribution if and only if significant depopulation occurs. The general resemblance of the right-hand side of the distributions can be explained through the temperature-induced sensitivity enhancement and does not constitute true state distribution changes. Also, under an illumination intensity of the order of several microwatts, there is no significant split of the two quasi-Fermi levels and thus no effect on the energy distribution.

As predicted by theory and substantiated by experiment, band-gap broadening is observed with decreasing temperature. This broadening is called the ''spectral blueshift'' of the band gap (shown in Figs. 2 and 3 by a dashed line, connecting the band-to-band transitions at different temperatures). The broadening is consistent throughout the temperature range. The semiempirical formula for the temperature-dependent band gap, as derived previously by indirect measurements, is[17,18]

$$Eg(T) = Eg(0) - \frac{aT^2}{b+T}. \tag{3}$$

Here, $a = 4.1(\pm 0.3)\times 10^{-4}$ eV/K and $b = 136(\pm 60)$ K are correlation constants. $E_g(0) = 1.42$ eV is the InP estimated band gap at ~0 K.[19] A good correlation to the measurements was achieved.[11,12,13] The maximum discrepancy is less than 0.01 eV, i.e., <1% of the band-gap value at room temperature (1.35 eV).

IV. CONCLUSIONS

In conclusion, T-SPS provides detection of midgap states, not active at room temperature, a semiempirical methodology for obtaining a partial description of a midgap state distribution, and an accurate method for directly observing spectral blueshift.

T-SPS reveals a gap state, attributed to Fe unintentional

doping, situated 0.79 eV below the conduction-band minimum. The energy distribution of this state has been investigated by measuring its population as a function of temperature and shows good agreement with theory. A direct observation of the spectral blueshift of the InP band gap by *T*-SPS shows very good agreement with theory.

ACKNOWLEDGMENTS

We would like to thank Dr. L. Kronik for consultations and illuminating remarks. Y.S. is grateful to Dinah and Henry Krongold for their generous support.

APPENDIX A: THE RELATION BETWEEN SPV AND POPULATION OF A GAP STATE

According to Kronik and Shapira,[9] the population concentration of a deep-level local state can be approximated by

$$n_t = \frac{C_n n_b e^{qV_S/kT} + C_p p_1}{C_n(n_b e^{qV_S/kT} + n_1) + C_p(p_b e^{-qV_S/kT} + p_1)} N_t \tag{A1}$$

We assume $n_b \approx n_i^2(T)/N_A \ll p_b \approx N_A$ (which, for $N_A = 6.7 \times 10^{16}$ cm^{-3}, is safe to assume). Thus we obtain

$$\frac{n_t}{N_t} = \frac{C_p p_1}{C_n n_1 + C_p(N_A e^{-qV_S/kT} + p_1)}. \tag{A2}$$

Substituting

$$n_1 = 2\left(\frac{2\pi m_e^* k}{h^2}\right)^{3/2} T^{3/2} \exp\left(\frac{E_t - E_C}{kT}\right),$$

$$p_1 = 2\left(\frac{2\pi m_h^* k}{h^2}\right)^{3/2} T^{3/2} \exp\left(\frac{E_V - E_t}{kT}\right)$$

calculated for *bulk* properties into Eq. (A2) yields

$$\frac{n_t}{N_t} = \frac{2C_p\left(\frac{2\pi m_h^* k}{h^2}\right)^{3/2} T^{3/2} e^{(E_V - E_t)/kT}}{2C_n\left(\frac{2\pi m_e^* k}{h^2}\right)^{3/2} T^{3/2} e^{(E_t - E_C)/kT} + C_p\left[N_A e^{-qV_S/kT} + 2\left(\frac{2\pi m_h^* k}{h^2}\right)^{3/2} T^{3/2} e^{(E_V - E_t)/kT}\right]}. \tag{A3}$$

To simplify the expression, we abbreviate the constants:

$$a = 2C_p\left(\frac{2\pi m_h^* k}{h^2}\right)^{3/2}, \quad b = 2C_n\left(\frac{2\pi m_e^* k}{h^2}\right)^{3/2}, \quad \text{and}$$

$$c = C_p N_A.$$

Substituting them into Eq. (A3) yields

$$\frac{n_t}{N_t} = \frac{aT^{3/2} e^{(E_V - E_t)/kT}}{bT^{3/2} e^{(E_t - E_C)/kT} + ce^{-qV_S/kT} + aT^{3/2} e^{(E_V - E_t)/kT}}. \tag{A4}$$

Since the exponents $e^{E_V - E_t/kT}$ and $e^{E_t - E_C/kT}$ do not change appreciably inside the temperature range (80–300 K), one can consign them to variables that are weakly temperature dependent:

$$\alpha(T) = ae^{(E_V - E_t)/kT},$$

$$\beta(T) = be^{(E_t - E_C)/kT},$$

$$\gamma(T) = ce^{-qBB/kT}.$$

The gamma variable is due to $V_S = BB + SPV(T)$. Here, V_S is the surface band bending, under steady-state illumination conditions. BB is the surface band bending under thermal equilibrium, before illumination.

Thus, when substituted into Eq. (A4), the result is

$$\frac{n_t}{N_t} = \frac{\alpha(T)T^{3/2}}{\beta(T)T^{3/2} + \gamma(T)e^{-qSPV(T)/kT} + \alpha(T)T^{3/2}}. \tag{A5}$$

Using $\delta(T) = \alpha(T) + \beta(T)$ results in

$$\frac{n_t}{N_t} = \frac{\alpha(T)T^{3/2}}{\delta(T)T^{3/2} + \gamma(T)e^{-qSPV(T)/kT}}. \tag{A6}$$

This expression links our SPV measurements of the S_2 state to its normalized population as a function of temperature.

We extracted a typical S_2 state SPV magnitude as a function of temperature. The values $E_V - E_t \approx -0.033$ eV and $E_t - E_C \approx -1.366$ eV were extracted from our experiment analysis and treated as constants throughout the temperature range. One must consider that a *surface* state, situated near midgap, does not necessarily reside in midgap relative to the bulk valence and conduction bands (outside the space-charge region). Using the cross-section data $C_p = 8 \times 10^{-18}$ cm^{-2} and $C_n = 9 \times 10^{-18}$ cm^{-2} obtained by Singh and Anderson,[20] a numeric calculation is possible. The first energy-based derivative of Eq. (A6) yields the state energy distribution. This derivative was correlated to the S_2 SPV signal, taken at 1 eV, throughout the temperature range and translated to its energy-dependent description.

APPENDIX B: CALCULATION OF THE FERMI LEVEL AND VALENCE-BAND ENERGY POSITION, RELATIVE TO THE INTRINSIC FERMI LEVEL

The empirical formulation of the band-gap temperature-induced widening (spectral blueshift) is

$$E_g(T) = E_g(0) - \frac{aT^2}{b+T}. \tag{B1}$$

For InP $a=4.1(\pm 0.3)\times 10^{-4}$ eV/K, $b=136(\pm 60)$ K, and $E_g(0)=1.42$ eV.[18]

Thus, $E_V(T)$ with reference to E_i is

$$E_V(T)=-\frac{E_g(T)}{2}. \tag{B2}$$

The accurate expression for $E_V(T)$ is

$$E_V(T)=-\frac{1}{2}\left(E_g(0)-\frac{aT^2}{b+T}\right). \tag{B3}$$

The accurate Fermi-level displacement formulation is

$$E_F(T)-E_i=kT\ln\left(\frac{n_i(T)}{N_A^-(T)}\right). \tag{B4}$$

Thus, the intrinsic carrier concentration is needed. The intrinsic carrier concentration is given by

$$n_i(T)=4.9\times 10^{15}(m_e^* m_h^*)^{3/4}T^{3/2}e^{-Eg/2kT},$$

For InP, we get

$$n_i(T)=\underset{n_i(300)}{1.4\times 10^7}\left(\frac{T}{300}\right)^{3/2}\exp\left[-\frac{1}{2k}\left(\frac{E_g(T)}{T}-\frac{E_n(300)}{300}\right)\right]. \tag{B5}$$

Furthermore, since the samples are p type, it is necessary to calculate the acceptor ionization level:

$$N_A^-(T)=\frac{N_A}{1+\frac{1}{4}e^{[E_A-E_F(T)]/kT}}. \tag{B6}$$

Here, $N_A=6.7\times 10^{16}$ cm^{-3} and $E_A=0.0281$ eV for the Zn-doped samples.

The accurate calculation procedure involves asymptotic correlation between Eqs. (B4) and (B6). Such a calculation, with an error level of less than $\sim(1\times 10^{-5})\%$ was conducted.

An easier, more intuitive approach is using the assumption of total ionization of the Zn dopant throughout the temperature range (300–80 K). The resulting expression for the Fermi level is

$$E_F(T)-E_i=kT\ln\left(\frac{n_i(T)}{N_A}\right). \tag{B7}$$

A correlation between the methods yields excellent agreement. Thus, one can use N_A instead of N_A^- to simplify calculations of the Fermi-level position displacement as a function of temperature.

Combining Eqs. (B7) and (B3), one gets the relative displacement between them:

$$E_F(T)-E_V(T)=kT\ln\left(\frac{n_i(T)}{N_A}\right)+\frac{1}{2}\left(E_g(0)-\frac{aT^2}{b+T}\right) \tag{B8}$$

*Corresponding author. Email address: shapira@eng.tau.ac.il

[1] S. E. Rosenbaum, B. K. Kormanyos, L. M. Jelloian, M. Matloubian, A. S. Brown, L. E. Larson, L. D. Nguyen, M. A. Thompson, L. P. B. Katehi, and G. M. Rebeiz, IEEE Trans. Microwave Theory Tech. **43**, 927 (1995).

[2] M. Hamacher, D. Trommer, K. Li, H. Schroeter-Jansen, W. Rehbien, and H. Heidrich, IEEE Photonics Technol. Lett. **8**, 75 (1996).

[3] X. Duan, Y. Huang, Y. Cui, J. Wang, and C. M. Lieber, Nature (London) **409**, 66 (2000).

[4] G. Raghavan, M. Sokolich, and W. E. Stanchina, IEEE Spectrum **37**, 47 (2000).

[5] S. A. Ringel, Solid-State Electron. **41**, 359 (1997).

[6] W. G. Schmidt, F. Bechstedt, and G. P. Srivastava, Surf. Sci. Rep. **25**, 141 (1996).

[7] L. Eldada, Opt. Eng. **40**, 1165 (2001).

[8] E. G. Guk, A. V. Kamanin, N. M. Shmidt, V. B. Shuman, and T. A. Yurre, Semiconductors **33**, 265 (1999).

[9] L. Kronik and Yoram Shapira, Surf. Sci. Rep. **37**, 1 (1999).

[10] J. Lagowski, C. L. Balestra, and H. C. Gatos, Surf. Sci. **29**, 213 (1972).

[11] N. Kinrot, Yoram Shapira, and M. A. Bica de-Moraes, Appl. Phys. Lett. **70**, 3011 (1997).

[12] Yoram Shapira, L. J. Brillson, and A. Heller, J. Vac. Sci. Technol. A **1**, 766 (1983).

[13] L. J. Brillson and Yoram Shapira, Appl. Phys. Lett. **43**, 174 (1983).

[14] L. Burstein and Yoram Shapira, Semicond. Sci. Technol. **8**, 1724 (1993).

[15] C. E. Goodman, B. W. Wessels, and P. G. P. Ang, Appl. Phys. Lett. **45**, 442 (1984).

[16] M. Leibovitch, L. Kronik, E. Fefer, and Yoram Shapira, Phys. Rev. B **50**, 1739 (1994).

[17] M. A. Sze, *Physics of Semiconductor Devices* (Wiley, New York, 1981), pp. 22–25.

[18] R. K. Ahrenkiel and A. R. Adams, *Properties of Indium Phosphide* (Gresham, Old Working, 1991), pp. 25–28, 75, 98, 234–235.

[19] Z. Hang, H. Shen, and F. H. Pollak, Solid State Commun. **73**, 15 (1990).

[20] A. Singh and W. A. Anderson, J. Appl. Phys. **64**, 3999 (1988).